

# A transient shear stress model for the analysis of laminar water-hammer problems

## Un modèle des contraintes transitoires pour l'analyse des problèmes de coup de bélier laminaire

RICARDO A. PRADO, *Depto. de Mecánica Aplicada, Facultad de Ingeniería, Universidad Nacional del Comahue, calle Buenos Aires 1400, (8300) Neuquén - Argentina*

AXEL E. LARRETEGUY, *Depto. de Matemática y Métodos Cuantitativos, Universidad Argentina de la Empresa, Lima 717, (1073) Buenos Aires - Argentina*

### ABSTRACT

A transient shear stress model for the solution of water-hammer problems for laminar flow in pipes is presented. The model is based on the polynomial expansion of the radial profiles of axial velocities, and the solution of the resulting set of equations by the method of characteristics.

This approach, as compared to the usual quasi-steady model (which can be regarded as a particular case of the new method), allows for a better representation of the shear stress at the wall during the pressure transients.

The present model can be included with only minor modifications into any existing code for solving water-hammer problems that uses the characteristics method and the quasi-steady model.

The test of the new model against experimental results of Holmboe and Rouleau, given in [8], and mathematical models and numerical simulations of other authors [5][8] show that it is less cpu and memory demanding, and is able of obtaining comparable results.

### RÉSUMÉ

On présente un modèle des contraintes transitoires pour résoudre les problèmes de coup de bélier dans les écoulements laminaires en tuyaux. Le modèle est basé sur le développement polynomial des profils radiaux de vitesses axiales, et la résolution du système d'équations obtenu, par la méthode des caractéristiques. Cette approche, par comparaison avec le modèle quasi-stationnaire habituel (qui peut être vu comme un cas particulier de la nouvelle méthode) permet une meilleure représentation de la contrainte pariétale pendant les transitoires de pression. Le présent modèle peut être inclus, moyennant des modifications mineures, dans tout code existant résolvant les problèmes de coup de bélier par la méthode des caractéristiques avec le modèle quasi-stationnaire.

Les tests du nouveau modèle faits sur les résultats expérimentaux de Holmboe et Rouleau, donnés en [8], et sur les modèles mathématiques et les simulations numériques d'autres auteurs [5][8], montrent qu'il consomme moins de temps cpu et de mémoire pour des résultats comparables.

### Introduction

The usual way of solving a water-hammer problem is to represent the unsteady viscous stress on the pipe wall with a model similar to that used for steady flow. That is, it is assumed that the shear stress at the wall is proportional only to the local mean velocity; this is the so-called *quasi-steady model*.

However, due to the very presence of pressure waves that travel along the pipe, the instantaneous velocity profiles found during the transient are far from being parabolic. The discrepancies turn to be more important next to the pipe wall, where the Richardson's effect [6] is present. Due to this, the quasi-steady model does a poor job in modeling the shear stress at the wall.

To overcome this difficulty, more complex models have been proposed in the past, e.g. those of Zielke [8] and Vardy and Hwang [5]. Both models, like the one we are proposing in the present work, rely on the method of characteristics for solving the resulting set of equations. The model of Zielke is based on the solution of a 1D problem in which the wall shear stress in transient laminar pipe flow is related to the instantaneous mean velocity and to weighted past velocity changes; therefore, this method requires that the history of all the previously calculated nodal velocities be kept in storage. On the other hand, Vardy and Hwang propose a quasi two-dimensional model by discretizing the do-

main in a set of concentric cylindrical annuli, and solving a water-hammer problem for each of them.

In the following, a new model for calculating the shear stress at the wall for transient laminar pipe flow is proposed. The model is based on the polynomial expansion of the radial velocity profiles, and the solution of the resulting set of equations by the method of characteristics.

In the rest of the paper, the idea behind the mathematical model, and the model itself, is described. The governing equations are then rewritten in the characteristic form of the partial differential equations, as is usual in solving this kind of problems, and the resulting system is discretized and solved by means of a Finite Difference formulation [1]. Finally, the results obtained with the proposed model are compared against numerical results obtained by other authors [5][8] and experimental results of Holmboe and Rouleau, taken from reference [8].

### Mathematical model

#### Motivation

In references [3] and [4], Prado and Marchegiani solved a transient problem which is close to a water-hammer problem in a pipe. They considered an infinite pipe, and imposed a given time-

Revision received September 15, 2000. Open for discussion till August 31, 2002.

dependent pressure gradient along the pipe axis that resembles the pressure histories obtained by Zielke in [5]. Prado and Marchegiani solved an unsteady axisymmetric problem to obtain the instantaneous axial velocity profiles,  $v(r,t)$ , as a function of the radial position,  $r$ , and time,  $t$ , in a section of the pipe. They proceeded by discretizing the Navier-Stokes equations in  $r$  and  $t$  via Finite Differences. An example of the resulting velocity profiles, for five different times, is shown in Fig.1. The five times are  $t = \{t^*, t^*+T/4, t^*+T/2, t^*+3T/4, t^*+T\}$ , where  $t^*=L/(2a)$  is the time the first pressure wave takes to arrive to the position  $z = L/2$ , and  $T = 4L/a$  the period of the wave (for the original problem of [5]).

The shape of these profiles led the present authors to the idea that they may be represented by a polynomial expansion in  $r$  with reasonable accuracy. This is the key idea behind the method we present below. In fact, the usual way of solving this kind of problems is the quasi-steady model, involving the expansion of  $v(r,t)$  into a polynomial with only one term, that of degree 2, and thus it may be regarded as a special case of the new method.

### Water-hammer governing equations

Under the following assumptions:

- horizontal rigid pipe of constant radius,  $R$ ,
  - purely axial flow,
  - constant pressure distribution across the pipe section,
  - flow velocity,  $V$ , negligible with respect to the fluid speed of sound,  $a$ , and
  - negligible viscous normal stresses,
- the approximated (i.e. integrated in  $r$ ) equations for the water-hammer phenomenon are reduced to the following hyperbolic system of two coupled partial differential equations for the static pressure,  $p(z,t)$ , and the mean velocity,  $V(z,t)$ , as functions of position along the pipe axis,  $z$ , and time,  $t$

$$\frac{\partial p}{\partial t} + \rho a^2 \frac{\partial V}{\partial z} = 0, \quad (1.a)$$

$$\frac{\partial V}{\partial t} + \frac{1}{\rho} \frac{\partial p}{\partial z} - S = 0 \quad (1.b)$$

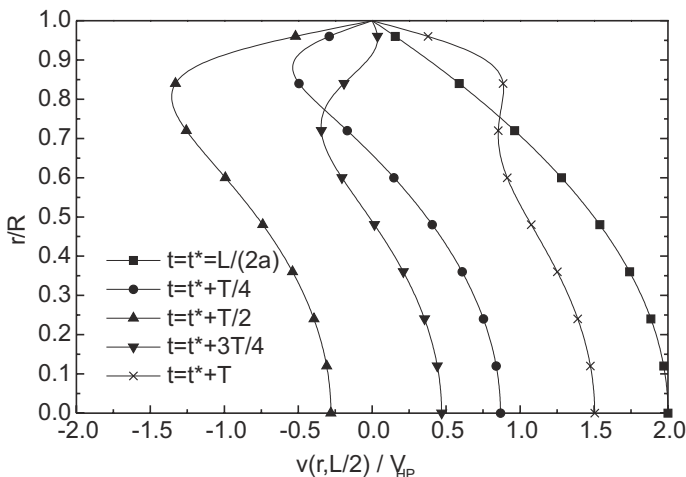


Fig. 1 example of velocity profiles obtained by Prado and Marchegiani [3][4]

where  $\rho$  denotes the fluid density.

The following source term,  $S$ , comes from the integration on the pipe section of the viscous term

$$S = v \frac{\int_A \frac{1}{r} \frac{\partial}{\partial r} \left( r \frac{\partial v}{\partial r} \right) dA}{\int_A dA} = v \frac{\int_0^R \frac{\partial}{\partial r} \left( r \frac{\partial v}{\partial r} \right) dr}{\int_0^R r dr} \quad (2)$$

$$= \frac{v}{R^2} \frac{\int_0^1 \frac{\partial}{\partial \bar{r}} \left( \bar{r} \frac{\partial v}{\partial \bar{r}} \right) d\bar{r}}{\int_0^1 \bar{r} d\bar{r}} = \frac{2v}{R^2} \int_0^1 \frac{\partial}{\partial \bar{r}} \left( \bar{r} \frac{\partial v}{\partial \bar{r}} \right) d\bar{r}$$

where  $\nu$  denotes the fluid kinematic viscosity,  $\bar{r} = r/R$  the nondimensional radial coordinate, and  $v(r,z,t)$  the instantaneous velocity profile of the axial flow.

On the other hand, the mean velocity,  $V$ , is defined by the cross-sectional average rate of flow

$$V(z,t) = \frac{\int_A v(r,z,t) dA}{\int_A dA} = \frac{\int_0^R v r dr}{\int_0^R r dr} = \frac{\int_0^1 v \bar{r} d\bar{r}}{\int_0^1 \bar{r} d\bar{r}} = 2 \int_0^1 v(\bar{r}, z, t) \bar{r} d\bar{r} \quad (3)$$

In the quasi-steady model, for instance, the source term  $S$  is evaluated as

$$S = -f \frac{|V|V}{4R}, \quad (4)$$

where Darcy's and Weissbach's friction factor,  $f$ , is calculated assuming that the velocity profile is always parabolic, namely

$$f = 32 \frac{\nu}{VR}. \quad (5)$$

Therefore, for the quasi-steady model,  $S$  is only a function of the mean velocity,  $V$ , for a given pipe geometry and flowing fluid, that is,  $S = S(V)$ .

### Proposed model

In order to achieve a better representation of the unsteady shear stress at the wall, a more realistic representation of the local instantaneous velocity profiles must be considered.

If the axial flow is considered axisymmetric, the instantaneous axial velocity profiles,  $v = v(r,z,t)$ , may be expanded into a polynomial of the nondimensional radial coordinate,  $\bar{r}$ , in the form

$$v(\bar{r}, z, t) = \sum_{j \in J} a_j(z, t) [1 - \bar{r}^j], \quad (6)$$

where the coefficients  $a_j$  will be defined below, and where the set  $J$  is a user selected set of natural numbers, defined by  $J = \{j|j \in \mathbb{N}, j \geq 2\}$ . Eq.(6) automatically verifies the non-slip condition at the

wall, i.e. at  $\bar{r}$ , and should be chosen so as to be able to represent also the stationary laminar condition (Hagen-Poiseuille flow), i.e.

$$v_{HP}(\bar{r}) = 2V(1 - \bar{r}^2). \quad (7)$$

Due to that reason, the power  $j=2$  should always be present. The remaining powers are proposed in order to better represent Richardson's effect due to the oscillating pressure gradients.

On the other hand, we define the following additional, weighted averaged, velocities

$$\begin{aligned} V_i = V_i(z, t) &= \frac{\int_A v(r, z, t) \cdot r^i \cdot dA}{\int_A r^i \cdot dA} = \frac{\int_0^R v r^{i+1} dr}{\int_0^R r^{i+1} dr} = \frac{\int_0^1 v \bar{r}^{i+1} d\bar{r}}{\int_0^1 \bar{r}^{i+1} d\bar{r}} \\ &= (i+2) \int_0^1 v(\bar{r}, z, t) \bar{r}^{i+1} d\bar{r}, \end{aligned} \quad (8)$$

where  $i = 0, 1, 2, \dots, \dim(J)-1$ . It is obvious that for  $i = 0$ ,  $V_0(z, t) = V(z, t)$ , so that the "order zero velocity" is coincident with the flow cross section averaged velocity.

Once the set  $J$  is defined, the coefficients  $a_j(z, t)$  are determined (as functions of  $V_i$ ) as follows. To do this, Eq.(6) is replaced into Eq.(8), giving

$$\begin{aligned} V_i &= (i+2) \int_0^1 v(\bar{r}, z, t) \bar{r}^{i+1} d\bar{r} \\ &= \left\{ (i+2) \int_0^1 \left[ \sum_{j \in J} a_j (1 - \bar{r}^j) \right] \bar{r}^{i+1} d\bar{r} \right\} = \sum_{j \in J} G_{ij} a_j, \end{aligned} \quad (9)$$

where the matrix  $G_{ij}$  is defined by

$$G_{ij} = (i+2) \int_0^1 (1 - \bar{r}^j) \bar{r}^{i+1} d\bar{r} = 1 - \frac{(i+2)}{(i+j+2)}. \quad (10)$$

Therefore, the coefficients  $a_j$  are defined by

$$a_j = \sum_{i=0}^{\dim(J)-1} G_{ji}^{-1} V_i. \quad (11)$$

It should be noted that the index  $j$  is not a complete sequence of natural numbers, and therefore the matrix notation of Eqs.(9) to (11), and other equations below, are somehow an abuse of notation. The meaning of them is, nevertheless, quite clear, although care must be taken when implementing these equations in a computer code.

From the instantaneous velocity profile, the laminar shear stress,  $\tau$ , can also be determined (for a Newtonian fluid) as,

$$\begin{aligned} \tau(r, z, t) &= \mu \frac{\partial v}{\partial r} = \frac{\mu}{R} \frac{\partial v}{\partial \bar{r}} = -\frac{\mu}{R} \sum_{j \in J} j a_j \bar{r}^{j-1} \\ &= -\frac{\mu}{R} \sum_{i=0}^{\dim(J)-1} \left[ \sum_{j \in J} j G_{ji}^{-1} \bar{r}^{j-1} \right] V_i(z, t), \end{aligned} \quad (12)$$

where  $\mu$  denotes the viscosity of the fluid. At the wall  $\bar{r} = 1$ , and then

$$\begin{aligned} \tau_w(z, t) &= -\frac{\mu}{R} \sum_{j \in J} j a_j \\ &= -\frac{\mu}{R} \sum_{i=0}^{\dim(J)-1} \left[ \sum_{j \in J} j G_{ji}^{-1} \right] V_i(z, t). \end{aligned} \quad (13)$$

Consequently, the present model considers that the shear stress at the wall,  $\tau_w$ , is not only a function of the mean velocity, but also a function of the weighted-averaged velocities,  $V_i$ . These velocities should verify additional equations and give a better representation of the instantaneous local velocity profile, despite the fact that they are calculated as integrated terms.

#### Additional governing equations

Under the assumptions (a) to (e), the axial momentum equation for the laminar flow of a Newtonian fluid along a horizontal rigid pipe of constant radius is reduced to

$$\rho \frac{\partial v}{\partial t} + \frac{\partial p}{\partial z} - \mu \left[ \frac{1}{r} \frac{\partial}{\partial r} \left( r \frac{\partial v}{\partial r} \right) \right] = 0. \quad (14)$$

When Eq.(14) is multiplied by  $r^i$ , for  $i = 0, 1, 2, \dots, \dim(J)-1$ , and integrated on the cross sectional area,  $A$ , of the pipe, it follows

$$\int_A \left\{ \frac{\partial v}{\partial t} r^i + \frac{1}{\rho} \frac{\partial p}{\partial z} r^i - v \left[ \frac{1}{r} \frac{\partial}{\partial r} \left( r \frac{\partial v}{\partial r} \right) \right] r^i \right\} dA = \int_A 0 dA = 0. \quad (15)$$

Again, under the assumptions (a) to (e), the derivatives can be taken out of the integrals, giving

$$\frac{\partial}{\partial t} \left( \int_A v r^i dA \right) + \frac{1}{\rho} \frac{\partial p}{\partial z} \int_A r^i dA - v \int_A \frac{1}{r} \frac{\partial}{\partial r} \left( r \frac{\partial v}{\partial r} \right) r^i dA = 0, \quad (16)$$

and, dividing by  $\int_A r^i dA$ ,

$$\frac{\partial}{\partial t} \left( \frac{\int_A v r^i dA}{\int_A r^i dA} \right) + \frac{1}{\rho} \frac{\partial p}{\partial z} - v \frac{\int_A \frac{1}{r} \frac{\partial}{\partial r} \left( r \frac{\partial v}{\partial r} \right) r^i dA}{\int_A r^i dA} = 0. \quad (17)$$

Using the definition of  $V_i$ , Eq(8), this last equation may be rewritten in a form that resembles that of Eq.(1.b), that is

$$\frac{\partial V_i}{\partial t} + \frac{1}{\rho} \frac{\partial p}{\partial z} - S_i = 0, \quad (18)$$

where we introduce the sources

$$S_i = \mathbf{v} \frac{\int_A \frac{\partial}{\partial r} \left( r \frac{\partial v}{\partial r} \right) r^{i-1} dA}{\int_A r^i dA} = \frac{\mathbf{v}}{R^2} \frac{\int_0^1 \frac{\partial}{\partial \bar{r}} \left( \bar{r} \frac{\partial v}{\partial \bar{r}} \right) \bar{r}^i d\bar{r}}{\int_0^1 \bar{r}^{i+1} d\bar{r}} \quad (19)$$

$$= \frac{(i+2)\mathbf{v}}{R^2} \int_0^1 \frac{\partial}{\partial \bar{r}} \left( \bar{r} \frac{\partial v}{\partial \bar{r}} \right) \bar{r}^i d\bar{r},$$

for  $i=0,1,2,\dots,\dim(J)-1$ . Since during the transient the instantaneous velocity profile is assumed to verify the polynomial representation given by Eq.(6), we can replace this equation into Eq.(19), to obtain

$$S_i = \frac{(i+2)\mathbf{v}}{R^2} \int_0^1 \frac{\partial}{\partial \bar{r}} \left( \bar{r} \frac{\partial v}{\partial \bar{r}} \right) \bar{r}^i d\bar{r} \quad (20)$$

$$= \sum_{j \in J} \left[ \frac{(i+2)\mathbf{v}}{R^2} \int_0^1 \frac{\partial}{\partial \bar{r}} \left( \bar{r} \frac{\partial (1-\bar{r}^j)}{\partial \bar{r}} \right) \bar{r}^i d\bar{r} \right] a_j = \sum_{j \in J} H_{ij} a_j,$$

where the matrix  $H_{ij}$  can be easily evaluated, resulting

$$H_{ij} = \frac{(i+2)j^2\mathbf{v}}{(i+j)R^2}. \quad (21)$$

Therefore, after Eqs.(11) and (20), the sources  $S_i$  are found to be functions of all the velocities  $V_k$ , in the following way

$$S_i(z,t) = \sum_{j \in J} \sum_{k=0}^{\dim(J)-1} H_{ij} G_{jk}^{-1} V_k. \quad (22)$$

By combining Eq.(18) with Eqs.(1), and recalling that  $V_0 = V$ , the following hyperbolic system of partial differential equations is obtained

$$\frac{\partial p}{\partial t} + \rho a^2 \frac{\partial V_0}{\partial z} = 0, \quad (23.a)$$

$$\frac{\partial V_0}{\partial t} + \frac{1}{\rho} \frac{\partial p}{\partial z} - S_0 = 0, \quad (23.b)$$

$$\frac{\partial V_i}{\partial t} + \frac{1}{\rho} \frac{\partial p}{\partial z} - S_i = 0 \quad ; \quad i = 1, 2, \dots, \dim(J) - 1, \quad (23.c)$$

which can be rewritten as

$$\mathbf{I} \frac{\partial}{\partial t} \begin{Bmatrix} p \\ V_0 \\ \vdots \\ V_{\dim(J)-1} \end{Bmatrix} + \mathbf{B} \frac{\partial}{\partial z} \begin{Bmatrix} p \\ V_0 \\ \vdots \\ V_{\dim(J)-1} \end{Bmatrix} = \mathbf{E} \quad (24)$$

where  $\mathbf{I}$  is the identity matrix, and

$$\mathbf{B} = \begin{bmatrix} 0 & \rho a^2 & \dots & 0 \\ 1/\rho & 0 & & 0 \\ \vdots & & \ddots & 0 \\ 1/\rho & 0 & 0 & 0 \end{bmatrix} \quad \mathbf{E} = \begin{Bmatrix} 0 \\ S_0 \\ \vdots \\ S_{\dim(J)-1} \end{Bmatrix}. \quad (25)$$

The characteristic slopes in the  $(z,t)$  plane,  $\zeta = dz/dt$ , given by  $\det[\mathbf{B}-\mathbf{I}\zeta] = 0$ , are

$$\zeta_{1,2} = \pm a, \quad \zeta_{3,\dots,\dim(J)+1} = 0. \quad (26)$$

We are now going to rewrite the system (23) as a system of ordinary differential equations. First, Eqs.(23.a) and (23.b) are to be replaced by the following ordinary differential equations along characteristic lines

$$\frac{dV_0}{dt} + \frac{1}{\rho a} \frac{dp}{dt} = S_0(V_0, V_1, \dots, V_{\dim(J)-1}) \quad \frac{dz}{dt} = +a, \quad (27.a)$$

$$\frac{dV_0}{dt} - \frac{1}{\rho a} \frac{dp}{dt} = S_0(V_0, V_1, \dots, V_{\dim(J)-1}) \quad \frac{dz}{dt} = -a. \quad (27.b)$$

Secondly, by subtracting Eq.(23.b) from Eq.(23.c) in order to eliminate the pressure gradient term,  $\frac{\partial p}{\partial z}$ , we get

$$\frac{\partial V_i}{\partial t} - \frac{\partial V_0}{\partial t} = S_i(V_0, V_1, \dots, V_{\dim(J)-1}) - S_0(V_0, V_1, \dots, V_{\dim(J)-1}); \quad (27.c)$$

$$i = 1, 2, \dots, \dim(J)-1,$$

which could as well be reinterpreted as a set of ordinary differential equations along characteristics of infinite slope, that is  $\frac{dz}{dt} = 0$ .

Finally, the resulting hyperbolic system of  $\dim(J)+1$  equations in the unknowns  $\{p, V_0, V_1, \dots, V_{\dim(J)+1}\}$  can be written as

$$\frac{dV_0}{dt} + \frac{1}{\rho a} \frac{dp}{dt} = S_0 \quad \frac{dz}{dt} = +a, \quad (28.a)$$

$$\frac{dV_0}{dt} - \frac{1}{\rho a} \frac{dp}{dt} = S_0 \quad \frac{dz}{dt} = -a, \quad (28.b)$$

$$\frac{dV_i}{dt} - \frac{dV_0}{dt} = S_i - S_0 \quad ; \quad i = 1, 2, \dots, \dim(J)-1 \quad \frac{dz}{dt} = 0. \quad (28.c)$$

## Numerical model

The system (28) is discretized by Finite Differences, remembering that the characteristic directions define the spatial scheme for the total derivatives (Fig. 2), resulting

$$V_0|_l^{n+1} - V_0|_{l-1}^n + \frac{1}{\rho a} (p|_l^{n+1} - p|_{l-1}^n) = S_0|_{l-1}^n \cdot \Delta t, \quad (29.a)$$

$$V_0|_l^{n+1} - V_0|_{l+1}^n - \frac{1}{\rho a} (p|_l^{n+1} - p|_{l+1}^n) = S_0|_{l+1}^n \cdot \Delta t, \quad (29.b)$$

$$V_i|_l^{n+1} - V_i|_l^n - (V_0|_l^{n+1} - V_0|_l^n) = (S_i|_l^n - S_0|_l^n) \cdot \Delta t; \\ i = 1, 2, \dots, \dim(J)-1, \quad (29.c)$$

where the indices  $n$  and  $l$  represent, respectively, the discretization in time and space.

The initial condition corresponds to a Hagen-Poiseuille flow (the Reynolds number  $Re = 2\bar{v}R/\nu$  is assumed to be less than 2100). That is

$$p(z) = \frac{dp}{dz}(z-L), \quad (30)$$

with

$$\frac{dp}{dz} = -8\mu V_{HP}/R^2. \quad (31)$$

For this profile, the weighted-average velocities result

$$V_i(z,0) = 4V_{HP} / (4+i) \quad ; \quad i = 0, 1, 2, \dots, \dim(J)-1, \quad (32)$$

where  $V_{HP}$  is the mean velocity of the initial Hagen-Poiseuille flow.

The boundary conditions, corresponding to the valve-pipe-reser-

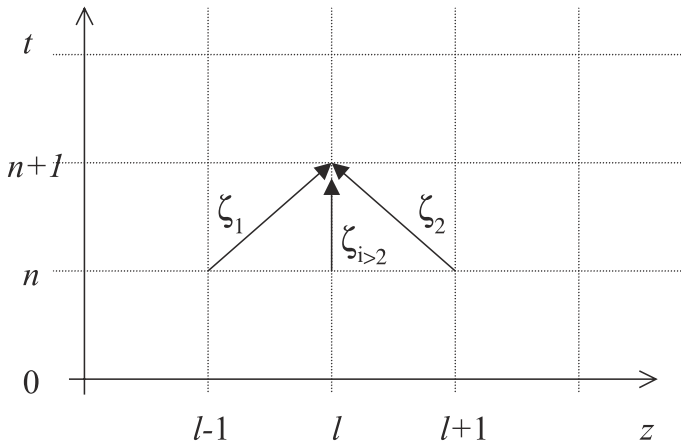


Fig. 2 Discretization and characteristic lines,  $\zeta$ , in the  $(z,t)$  plane

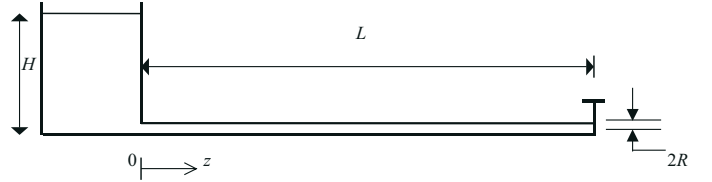


Fig. 3 Geometric configuration

voir configuration shown in Figure 3, and assuming a sudden valve closure, are

At the valve ( $z = L$ ):

$$V_0(L,t) = 0 \quad t > 0 \quad (33)$$

At the reservoir ( $z = 0$ ):

$$p(0,t) - \rho g H + \frac{1}{2} \rho [1 + K_R] V_0^2(0,t) = 0 \quad t > 0 \quad (34)$$

where  $K_R$  is the loss coefficient of the reservoir, and

$$H = \frac{(1 + K_R)}{2g} V_{HP}^2 + \frac{8\nu L}{gR^2} V_{HP}$$

denotes the height of the fluid in the reservoir, which is considered constant.

## Example and discussion of results

### Description

In order to show the results of the application of the present model, the experiment carried out by E.L. Holmboe and W.T. Rouleau, as described in [8], is reproduced. The experiment corresponds to the situation shown in Figure 3, in which the relevant parameters are the following:

- Pipe length,  $L = 36$  m,
- Pipe radius,  $R = 0.0127$  m,
- Kinematic viscosity,  $\nu = 39.67 \cdot 10^{-6}$  m<sup>2</sup>/s (at 27°C),
- Speed of sound,  $a = 1324.4$  m/s

The initial condition is a fully established Hagen-Poiseuille flow, with the valve completely open. At time  $t=0$ , the valve is suddenly closed.

The following values were considered for the loss coefficient of the reservoir,  $K_R$

$$K_R = \begin{cases} 1.0 & \text{if } V_0(0,t) \geq 0 \\ 0.5 & \text{if } V_0(0,t) < 0 \end{cases}$$

### Model options

The problem was solved for three different options, namely, (a), (b) and (c), which differ in the selection of the set  $J$ :

- a)  $J_a = \{2, 8, 12\}$
- b)  $J_b = \{2, 6, 10, 12\}$
- c)  $J_c = \{2, 3, 4, 5, 6, 7, 8, 9, 10, 11, 12\}$

All these sets need to have relatively high exponents (i.e. 10, 12)

in order to better represent the sharp variations in the slope of the velocity profiles near the wall. Obviously, they also need exponent 2 to represent the initial condition (Hagen-Poiseuille).

Options (a) and (b) are the better selections, in our experience, for solving the problem with small sets. Option (c) is, obviously, the complete set up to degree 12.

In the following, for each option, the source terms,  $S_i$ , result from Eq.(22), and the shear stress at the wall,  $\tau_w$ , from Eq.(13).

Option a:

$$S_0 = \frac{v}{R^2} 2(-280V_0 + 825V_1 - 576V_2) \quad (35)$$

$$S_1 = \frac{v}{R^2} \frac{4}{39} (-8050V_0 + 23925V_1 - 16752V_2) \quad (36)$$

$$S_2 = \frac{v}{R^2} 4(-278V_0 + 825V_1 - 576V_2) \quad (37)$$

$$\tau_w = \frac{\mu}{R} (280V_0 - 825V_1 + 576V_2) \quad (38)$$

Option b:

$$S_0 = \frac{v}{R^2} (1792V_0 - 8775V_1 + 13440V_2 - 6545V_3) \quad (39)$$

$$S_1 = \frac{v}{R^2} \frac{3}{2002} (1808128V_0 - 8818875V_1 + 13489280V_2 - 6564635V_3) \quad (40)$$

$$S_2 = \frac{v}{R^2} 2(1796V_0 - 8775V_1 + 13440V_2 - 6545V_3) \quad (41)$$

$$S_3 = \frac{v}{R^2} \frac{5}{2} (1792V_0 - 8769V_1 + 13440V_2 - 6545V_3) \quad (42)$$

$$\tau_w = \frac{\mu}{R} \frac{1}{2} (-1792V_0 + 8775V_1 - 13440V_2 + 6545V_3) \quad (43)$$

Option c:

Due to the large number of terms, this option is best represented in the following table:

Table I: coefficients for option c

	<i>Coeff.</i>	$V_0$	$V_1$	$V_2$	$V_3$	$V_4$	$V_5$	$V_6$	$V_7$	$V_8$	$V_9$	$V_{10}$
$S_0$	308 v/R <sup>2</sup>	-26	975	-14040	106080	-477360	1360476	-2519400	3023280	-2267460	965770	-178296
$S_1$	3 v/R <sup>2</sup>	-11858/3	298375/2	-2152920	16283960	-73324944	209065626	-387277000	464838990	-348691420	445613707/3	-356532568/13
$S_2$	8 v/R <sup>2</sup>	-2001	75075	-1081080	8168160	-36756720	104756652	-193993800	232792560	-174594420	74364290	-13728792
$S_3$	5 v/R <sup>2</sup>	-4004	150153	-2162160	16336320	-73513440	209513304	-387987600	465585120	-349188840	148728580	-27457584
$S_4$	12 v/R <sup>2</sup>	-2002	75075	-1081078	8168160	-36756720	104756652	-193993800	232792560	-174594420	74364290	-13728792
$S_5$	7 v/R <sup>2</sup>	-4004	150150	-2162160	16336325	-73513440	209513304	-387987600	465585120	-349188840	148728580	-27457584
$S_6$	16 v/R <sup>2</sup>	-2002	75075	-1081080	8168160	-36756717	104756652	-193993800	232792560	-174594420	74364290	-13728792
$S_7$	63 v/R <sup>2</sup>	-572	21450	-308880	2333760	-10501920	29930473	-55426800	66512160	-49884120	21246940	-3922512
$S_8$	20 v/R <sup>2</sup>	-2002	75075	-1081080	8168160	-36756720	104756652	-193993796	232792560	-174594420	74364290	-13728792
$S_9$	11 v/R <sup>2</sup>	-4004	150150	-2162160	16336320	-73513440	209513304	-387987600	465585129	-349188840	148728580	-27457584
$S_{10}$	24 v/R <sup>2</sup>	-2002	75075	-1081080	8168160	-36756720	104756652	-193993800	232792560	-174594415	74364290	-13728792
$\tau_w$	154 $\mu$ /R	26	-975	14040	-106080	477360	-1360476	2519400	-3023280	2267460	-965770	178296

where, for instance

$$S_0 = 308 \frac{v}{R^2} (-26 V_0 + 975 V_1 - 14040 V_2 + 106080 V_3 - 477360 V_4 + 1360476 V_5 - 2519400 V_6 + 3023280 V_7 - 2267460 V_8 + 965770 V_9 - 178296 V_{10})$$

## Results

In Figs. 4, 5, and 6, the time histories of pressures, shear stresses at the wall, and mean velocities, all of them at  $z = L/2$ , are shown in non-dimensional form. Similarly, Figure 7 shows the pressure history at the valve, i.e. at  $z = L$ . Whenever data are available,

results for the three options of the present model are compared against the experimental data of Holmboe & Rouleau taken from [8], the numerical model proposed by Zielke [8], and that of Vardy and Hwang [5].

Finally, Fig. 8 shows, as an example, the instantaneous velocity profiles at the middle of the pipe, i.e.  $v(r, L/2, t)$ , at times  $t = \{t^*, t^*+T/4, t^*+T/2, t^*+3T/4, t^*+T\}$ , where  $t^* = L/(2a)$  is the time the first pressure wave takes to arrive to the position  $z = L/2$ , and  $T = 4L/a$  is the period of the wave. These profiles, calculated with option (c) of the present model, were reconstructed from the nodal values of the weighted-average velocities,  $V_i$ , using Eqs.(11) and (6).

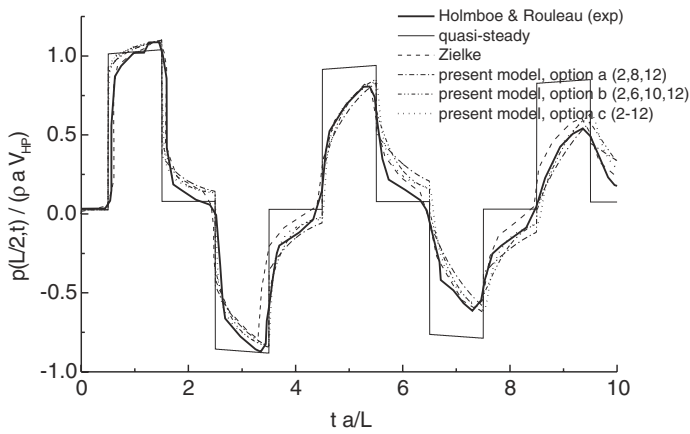


Fig. 4 pressure histories at  $z=L/2$

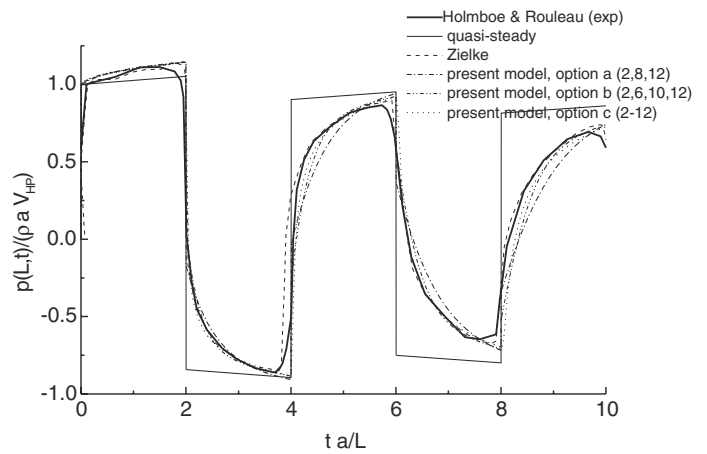


Fig. 7 pressure histories at the valve,  $z=L$

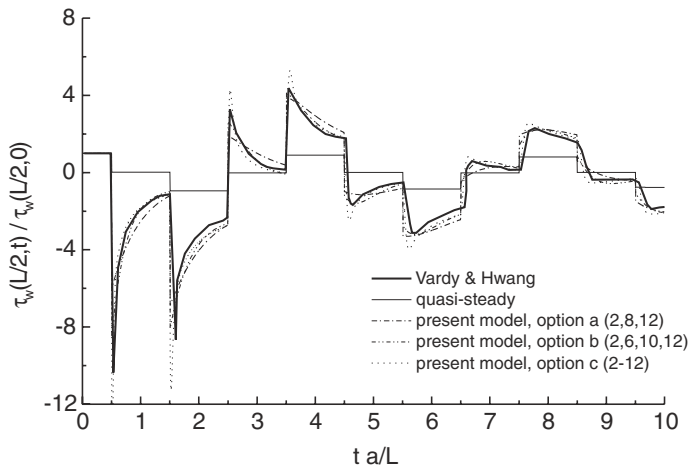


Fig. 5 wall shear stress at  $z=L/2$

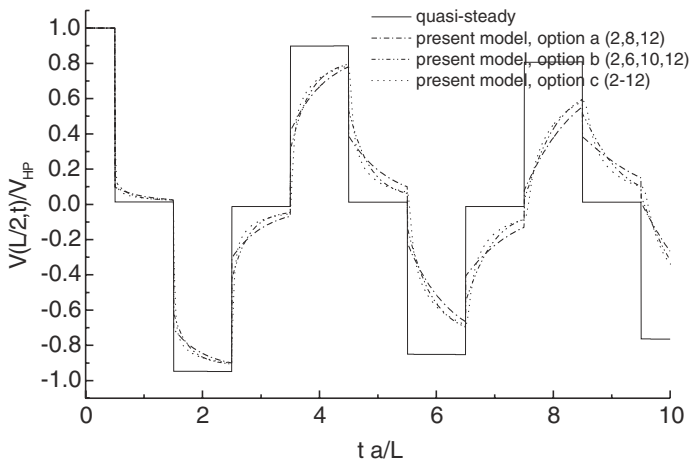


Fig. 6 mean velocity at  $z=L/2$

### Discussion of results

It is clear from Figs. 4 to 7 that the quasi-steady model provides a poor representation of the histories of all of the variables considered, a performance that is originated in the inability of adequately representing the wall shear stress.

Figs. 4 and 7 show that the three options of the present model considered here give pressure histories that are in good agreement with both experimental and Zielke's numerical results.

The wall shear stresses, shown in Fig. 5, also show good agreement between our results and Vardy's and Hwang's. Unfortunately, due to the nature of the variable considered, there are no experimental data to compare with. It should be taken into account that, as well as the present model results depend on the selection of the set  $J$ , Vardy's and Hwang's results depend on the number and distribution of the set of concentric cylindrical annuli. In particular, Vardy's and Hwang's results shown here correspond to a discretization composed by 24 cylinders.

Fig. 6 shows the dramatic difference in the histories of mean velocities obtained with the present model as compared to that obtained with the quasi-steady model.

### Comments

It should be stressed that, despite the differences found in the representation of the peak values of the wall shear stresses obtained with the three options (see Fig. 5), all the options give pressure and mean velocity histories that are close to each other. This would indicate that even small sets of only 3 or 4 terms, like the ones selected in options (a) and (b), should be enough for obtaining a good representation of the phenomena, far better than the usual quasi-steady approach. Moreover, the shear stress histories obtained for options (a) and (b) are also close to Vardy's and Hwang's results, which were obtained for a 24 cylinder discretization, thus indicating that the present model seems to be less computing demanding for comparable accuracy.

As a warning note, it is clear from the inspection of Table I, that the use of long complete sets gives rise to numbers prone to cause important round-off errors unless very high precision is used in the calculations. Therefore, the use of these "high-order" sets is discouraged, and, in our experience, unnecessary.

The velocity profiles shown in Fig. 8, although corresponding to a similar but not equal problem, clearly resemble that of Fig. 1 (and also agree with those of Fig. 7 of reference [5]). Consequently, the present model is also able to provide, as a by-product, a reasonable representation of the instantaneous velocity profiles at any point in the pipe.

It is worth noting that the present model can be included with minor modifications into any existing code for solving water-ham-

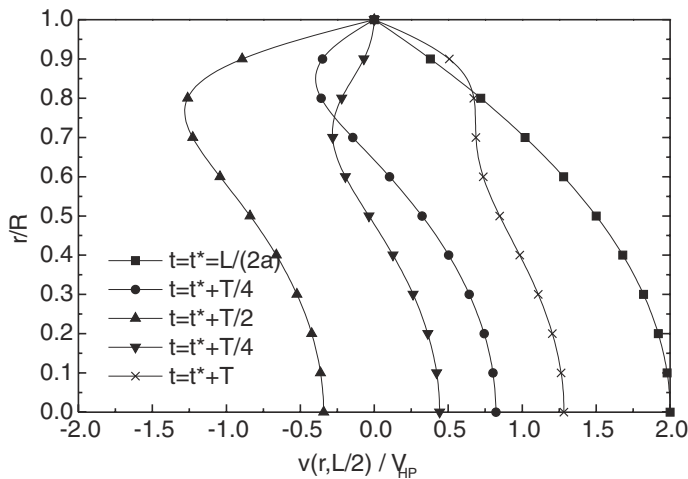


Fig. 8 velocity profiles at selected times, calculated with the present model (option c)

mer problems via the characteristics method, for it involves only the declaration of a few additional nodal variables (the  $V_i$ ), the evaluation of the sources  $S_i$ , and the consequent solution of the resulting set of linear algebraic equations in the new unknowns. Moreover, if the code is of a general nature, that is, if it can solve not only a single pipe but a complete network of pipes interconnected by different types of fittings (e.g. ref. [2]), no additional modifications other than that already described are required to implement the present model. Particularly, no boundary conditions need to be specified for the additional velocities, i.e.  $V_i$  for  $i > 0$ , for they are determined from their values in the past time step and the present value of  $V_0$  by means of Eq.(29.c). Additionally, no modifications are required in the models of the fittings.

## Conclusions

A model for the solution of water-hammer problems for laminar flow in pipes has been presented. The model is based on the polynomial expansion of the radial profiles of axial velocities, and the solution of the resulting set of equations by the method of characteristics. It provides information not only about pressures and mean velocities, but also the instantaneous axial velocity profiles and the shear stress at the wall.

This approach, as compared to the usual quasi-steady model, allows for a better representation of the shear stress at the wall during the pressure transients. In fact, the quasi-steady model is a particular case (the simplest and less-accurate one) of the new method.

The test of the present model against experimental results by Holmboe and Rouleau, given in [8], and mathematical models and numerical simulations of other authors [5][8] show that the present model is able of obtaining comparable results. Moreover, the present methodology results simpler and less memory demanding than that of reference [8], which requires the storage of the history of the motion. It is also expected to be less cpu demanding than models that require the discretization of the problem in the radial direction, i.e. reference [5].

Is important to note that the present model can be included with only minor modifications into any existing code for solving

water-hammer problems via the characteristics method and the quasi-steady model. This is true even for more involved codes able to solve not only a single pipe but a whole network of pipes interconnected by different types of fittings.

The present approach should also be able to deal with turbulent flows, although this would require the identification of a different set of exponents, or even the selection of an expansion other than into a polynomial one. This appears as the natural continuation of the present work.

## Acknowledgments

The authors wish to thank Dr. J.C. Ferreri for inspiring the present work.

## List of symbols

$a$	speed of sound, coefficient of interpolation
$A$	pipe section
$f$	Darcy's and Weissbach's friction factor
$g$	gravity acceleration
$J$	set of natural numbers
$K$	loss coefficient
$L$	length of pipe
$p$	static pressure
$r$	radial coordinate
$R$	radius of pipe
$S$	sources
$t$	time
$T$	period
$v$	axial velocity
$V$	average or weighted-average velocity
$z$	axial coordinate

## Greek symbols

$\nu$	kinematic viscosity
$\mu$	dynamic viscosity
$\rho$	density
$\tau$	shear stress

## Subindices/Supraindices

$i, k$	order of the term in the polynomial expansion
$j$	exponents of the polynomial expansion
$w$	pertaining to the wall
$HP$	Hagen-Poiseuille

## References

- [1] ANDERSON D.A., TANNEHILL J.C. and PLETCHER R.H.: "Computational Fluid Mechanics and Heat Transfer", Hemisphere Publishing Corporation, McGraw-Hill Book Company, 1984.
- [2] LARRETEGUY A., CARRICA P., BALIÑO J. and SANTA ANA P., "WHAT: Water-Hammer Analysis in Tubes V.1.0 - Us-

- ers Manual”, technical report CNEA/CAB 3509, August 1993.
- [3] PRADO R.A. and MARCHEGIANI A.R.: “Flujo tubular no permanente por presencia de trenes de ondas de presión”. *Mecánica Computacional*, Vol.XV, pp.285-294, 1995.
- [4] PRADO R.A. and MARCHEGIANI A.R.: “Discrepancias en la determinación de la tensión cortante en flujo tubular, bajo condiciones no estacionarias”. *Anales del VII Congreso Nacional de Ingeniería Mecánica*, Valdivia, Chile, pp.587-590, Octubre de 1996.
- [5] VARDY A.E. and HWANG K.L.: “A characteristics model of transient friction in pipes”, *Journal of Hydraulic Research*, Vol.29, No.5, pp.669-683, 1991.
- [6] WHITE F.M.: “Viscous Fluid Flow”, Second Edition, McGraw-Hill, Inc., 1991.
- [7] WYLIE E.B and STREETER V.L.: “Fluid Transients”, Corrected Edition 1983, FEB Press, USA.
- [8] ZIELKE W.: “Frequency-Dependent Friction in Transient Pipe Flow”, Paper No.67-WA/FE-15, 1967.